Conformations of Propargyl alcohol

And its Hydrogen Bonded Complexes with Water

Studied using Matrix Isolation Infrared Spectroscopy and Computations

Jyoti Saini

A dissertation submitted for the partial fulfilment of

BS-MS dual degree in Science

Indian Institute of Science Education and Research Mohali

April 2014

Certificate of Examination

This is to certify that the dissertation titled "Conformations of Propargyl alcohol and its Hydrogen Bonded Complexes with water studied using Matrix Isolation Infrared Spectroscopy and Computations", submitted by Ms. Jyoti Saini (Reg. No.MS09066) for the partial fulfilment of BS-MS dual degree programme of the Institute has been examined by the thesis committee duly appointed by the Institute. The committee finds the work done by the candidate satisfactory and recommends that the report be accepted.

Dr. P. Balanarayan Dr. K. R. Shamasundar Prof. K.S. Viswanathan
(Supervisor)

Dated: 25 April, 2014

DECLARATION

The work presented in this dissertation has been carried out by me under the guidance of Prof. K. S Viswanathan at the Indian Institute of Science Education and Research Mohali.

This work has not been submitted in part or in full for a degree, a diploma, or a fellowship to any other university or institute. Whenever contributions of others are involved, every effort is made to indicate this clearly, with due acknowledgement of collaborative research and discussions. This thesis is a bonafide record of original work done by me and all sources listed within have been detailed in the bibliography.

Jyoti Saini
(Candidate)
Dated: 25 April, 2014

In my capacity as the supervisor of the candidate's project work, I certify that above statements by the candidate are true to the best of my knowledge.

Prof. K.S. Viswanathan

(Supervisor)

ACKNOWLEDGEMENT

I express my deep sense of gratitude to Prof. K. S. Viswanathan for his advice, expert guidance, valuable suggestions, discussions and constant encouragement during the entire course of this work and preparation of the thesis. I have learnt and gained a lot from his knowledge and experience. I consider myself extremely fortunate to be a student under his guidance. I wish to interact with him in future.

I express my sincere thanks to the Master's thesis committee members for their valuable suggestions and comments during the committee meeting.

I have learnt almost all the matrix isolation experimental skills from Bishnu Prasad Kar, Gaurav Verma and Kapil.

I am thankful to my lab members Kanupriya, Ginny, Mariyam, Deepak, Vivek and Pankaj who accompanied me throughout this research work.

I thank each of my classmates as well as neighbouring lab members who provided a wonderful and friendly atmosphere to carry out research during the entire period. It is my pleasure to thank each and every member of the Department of Chemical sciences who have helped me in various ways during the course of investigation and research.

I wish to acknowledge the Computing Facility staff for providing me excellent facilities during the computational work.

I express my sincere gratitude to each of my family members for their encouragement and moral support throughout the course of study.

I would also like to acknowledge the 'Department of Science and Technology, India' for providing the INSPIRE fellowship.

LIST OF FIGURES

LIST OF TABLES

LIST OF ABBREVIATIONS USED IN THIS THESIS

PA	Propargyl alcohol
FT	Fourier Transform
UV	Ultra Violet
HF	Hartree-Fock
MP	Møller–Plesset perturbation theory
DFT	Density Functional Theory
BLYP	Becke-Lee-Yang-Parr
SCF	Self- Consistent Field
M06	Minnesota functional
ZPE	Zero point vibrational energy
BSSE	Basis Set Superposition Error
AIM	Atoms –in-molecules
CP	Critical point
NCI	Non-covalent interactions
AA	Allyl alcohol (prop-2-en-1-ol)
PC	Propargyl carbinol (but-3-yn-1-ol)
AC	Allyl carbinol (but-3-en-1-ol)
ICL-PAS	Intracavity laser photoacoustic spectroscopy

CONTENTS

Abstract

Among the weak interactions the hydrogen bond is one of the most interesting and abundant interactions that influences a variety of chemical and biochemical processes. The study of hydrogen bonding systems, using both experimental and theoretical methods, is therefore of considerable interest. Hydrogen bonding such as O-H···O, O-H···π, (acetylenic) C-H···O and C-H···π have drawn considerable attention. Another interesting aspect is the investigation of competitive hydrogen bonding in a molecule having multiple bonding sites.

Among the several experimental techniques, which have been used to study weak interactions, matrix isolation infrared spectroscopy, together with quantum chemical calculations is a powerful tool. The spectral linewidths of features in a matrix isolated technique being small allows for the identification of weak complexes and conformations.

Propargyl alcohol is an example of a molecule with multiple hydrogen bonding sites and thus, can act as proton donor (acetylenic C-H and O-H) as well as proton acceptors (O atom and π electron cloud), which eventually gives rise to a number of possible hydrogen bonded systems.

In this thesis, we have explored experimentally and computational the rich potential energy landscape of the propargyl alcohol-water system. The computational work was performed at M06, MP2 and B3LYP levels of theory using 6-311++G (d, p) basis set. Nine different geometries at the M06, nine at MP2 and eight at B3LYP level were obtained. Most of the structures at the different levels (M06, MP2 and B3LYP) were similar at all three levels. The O-H···O interaction has been observed as a dominating interaction followed by weak H···π interaction computationally in the ground state optimized at all three levels. These complexes were studied experimentally using the matrix isolation technique.

CHAPTER 1
INTRODUCTION

This chapter discusses the studies on hydrogen bonding and places the present work in context.

1.1 The Hydrogen Bond

A hydrogen bond is an example of an interaction between two permanent dipoles. The large difference in electronegativities between hydrogen and any of fluorine, nitrogen and oxygen, coupled with their lone pairs of electrons causes strong electrostatic forces between molecules.

The hydrogen bond is usually represented as A-H···B, where A is an atom with electronegativity greater than that of hydrogen (C, O, N, P, Se, F, Cl, Br and I) and B can be π or σ electron donor site (Lewis base).

There are two types of hydrogen bonds: 1) Intermolecular hydrogen bonding, where the association is between two different species to form a complex and 2) Intramolecular hydrogen bonding, where two or more groups within the same molecule are associated.

Hydrogen bond is weaker than a conventional chemical bond. Hydrogen bond energies between proton donor groups such as O-H or N-H (hard acids) and electronegative atoms such as O or N (hard bases) are within 3 to 10 kcal/mol.

The π cloud is a widely studied base for many proton accepting groups. Dewar first proposed, in 1944, that the π electron system could act as an electron donor.[1] The π cloud, a soft base, can interact with XH groups (X=C,O or N), to form a hydrogen bond, which is generally weaker than conventional hydrogen bonds.[2]

There are various instrumental and computational techniques, which can be employed to study weak hydrogen bonds; there are vibrational spectroscopy, gas phase rotational spectroscopy and computations, In this work we have used matrix isolation infrared spectroscopy to study hydrogen bonded complexes between propargyl alcohol (PA) and water. A detailed description of this technique has been provided in Chapter 2.

1.2 Status of current research

There have been previous experimental Microwave[3,4] and Infrared (IR) studies on propargyl alcohol[5] . The microwave spectrum of propargyl alcohol has confirmed the presence of only the gauche form.[3,4,6] Similarly only the gauche form has been observed for the analogous molecules propargyl thiol (C_3H_4S)[7-10] and propargyl selenol (C_3H_4Se)[11]. Hirota suggested that the extra stabilization of the syn or gauche conformer of PA may be due to Intramolecular interaction between the –OH group and π electrons.[3] A single OH-stretching band is observed in the Fundamental IR spectrum of PA, indicating that only one conformer is present.[5] The vibrational overtone spectra of propargyl alcohol (prop-2-yn-1-ol, PA), allyl alcohol (prop-2-en-1-ol, AA), propargyl carbinol (but-3-yn-1-ol, PC) and allyl carbinol (but-3-en-1-ol, AC) has also been recorded with intracavity laser photoacoustic spectroscopy (ICL-PAS) to study intramolecular hydrogen bonding interactions.[12]

However, subsequent theoretical investigations suggest that the lowest energy conformer of PA is not stabilized by an OH···π intramolecular hydrogen bond. [13] Atoms in molecules (AIM) studies have been carried out to analyse the interactions between the OH-group and the π-electrons of the carbon–carbon multiple bonds. These calculations have not shown a bond critical point between the hydroxyl proton and the π bond, in agreement with an earlier result.[12]

There have been several spectroscopic studies of propargyl alcohol, which have mainly focused on a vibration-rotation interaction and intramolecular vibrational energy redistribution in the ground electronic state. Frequency and time domain spectroscopic studies (Raman[14,15], high resolution IR[16,17], transient absorption spectroscopy[18]) of propargyl alcohol show fast energy redistribution from the initially excited acetylenic C-H stretching vibration, which was explained by the large number of bath states including vibration-rotation interaction with no special effect of low frequency OH torsional vibration.[19] Structures and dynamics of propargyl alcohol in the ground electronic state have widely been studied.[20-23]

PA offers many interesting possibilities of intermolecular interactions with other atoms/molecules; results have been reported on the first complex chosen for investigation, Ar···PA. Ab initio quantum chemical calculations were also carried out to optimize the structure of Ar···PA at the MP2/6-311+G(3df,2p) level.[24] Although there have been numerous studies on this interesting molecule, it appears that there have been no prior experimental as well as theoretical studies on any of its complexes.

1.3 Motivation for the Present Work

Molecules with multiple hydrogen bonding sites can provide the opportunity to investigate competitive hydrogen bonding. They can act as a proton donor or acceptor depending on the molecular species, with which they interact, and the environment. Such molecules with multiple hydrogen bonding sites form several closely spaced minima on the potential energy surface, which poses a challenge to study them experimentally.

In the present study, propargyl alcohol and water are chosen, since propargyl alcohol provides multiple hydrogen bonding sites. The active bonding sites are shown in **Figure 1**.

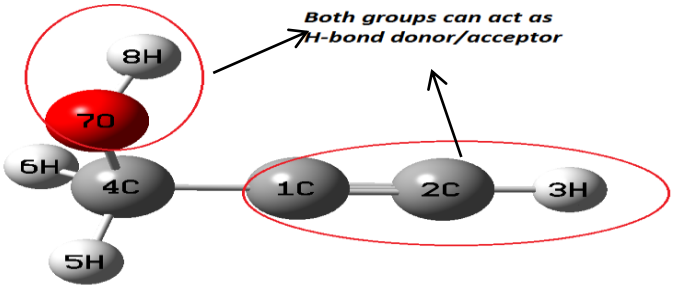

Figure 1- Structure of propargyl alcohol indicating the hydrogen bonding sites

In propargyl alcohol, both the O atom and π electron cloud can act as proton acceptor sites, whereas the acetylenic C-H and O-H can act as proton donor. These multiple sites offered by the precursor can be expected to show several minima.

Matrix isolation spectroscopy provides an excellent method to study the hydrogen bonded systems with multiple bonding sites as described above, as it is known to trap local minima.[25]

1.4 Scope and objective of the present work

This thesis will provide a report on the study of possible interactions between propargyl alcohol and water. In order to study these complexes experimentally, we have used Matrix Isolation Infrared Spectroscopy. Different computational methods have also been used to find out possible complexes between the two monomers propargyl alcohol and water. The experimentally observed features of the complexes were corroborated with ab initio computations.

CHAPTER 2
EXPERIMENTAL AND COMPUTATIONAL PROCEDURES

The present section deals with the experimental aspects of matrix isolation infrared spectroscopy and the computational methods which have been used to study the hydrogen bonded complexes of propargyl alcohol – water. This chapter discusses the instrumentation aspects of matrix isolation technique.

2.1 Matrix Isolation Technique

The matrix isolation method was first proposed for the experimental study of unstable molecules that has been described by Whittle, Dows, and Pimentel.[26] The technique consists of the dispersal of a chemically reactive material in a large excess of an inert solid substance (the matrix) at a temperature low enough to retard or prevent diffusion of the active molecules.[27] Although this technique was developed for the study of reactive species, this technique became a powerful tool to study the weakly bound complexes and conformations of molecules.

The sample of interest is first mixed with a large excess of an inert gas, such as argon or nitrogen and this mixture is then deposited on a cold substrate maintained at ~12K. The large excess of inert gas is used to ensure that the sample molecules are deposited, isolated from each other and thus, cannot interact with each other; typical matrix to sample ratios being 1000:1. Once the matrix-isolated sample molecules are prepared, one can easily probe them using any of the spectroscopic techniques such as infrared, electron spin resonance, UV-visible etc.

Among the various spectroscopic methods used to study the matrix isolated species, infrared spectroscopy has been widely used.[28]

2.2 Advantages

The spectrum obtained using the matrix isolation technique displays peaks with considerably smaller linewidths compared with the spectra recorded using liquid, gas or solid samples because the molecules of interest are isolated from each other in an inert

matrix and thus any intermolecular interactions between the sample molecules are significantly reduced. Also, the low temperature and rigid matrix cage constrain molecular motion leading to the elimination of Doppler and collisional broadening thus ensuring that only the lowest ro-vibronic and electronic levels of the molecule are populated.

2.3 Desirable Properties of a Matrix

The choice of a matrix material depends on the following properties:

1) It must be chemically inert and sufficiently rigid at low temperatures to prevent diffusion of the solute species. In addition, the matrix must also be suitable for accommodating the active molecules, either in lattice sites or in holes in the matrix.

2) It must primarily have sufficient vapour pressure at the room temperature to enable easy deposition of solute species.

3) It must also be easily available with a high degree of purity.

4) It should not have any absorption in the spectral wavelength region of interest. In addition to being non-absorbing, a suitable matrix must not scatter too large a fraction of the incident light.

Inert gases and nitrogen generally meet the above criteria and thus can be used as matrix gases. Among the inert gases argon is the most commonly used matrix gas.

While the matrix is considered to be inert towards the trapped solute species, in reality the matrix atoms may interact with the guest atoms in a variety of ways resulting in the spectrum of the trapped species being perturbed. Thus, it is essential to recognize these effects during the interpretation of the spectra. A very brief discussion of the various matrix effects and ways to identify these effects are presented in the following section. The matrix effects can be identified in a spectrum, as peak multiplets, shift in the peak position and broadening of the peaks.

2.4 Matrix shifts

The readily identified and the most common matrix effect is the frequency shift

from the gas phase value which arises from the electrostatic, inductive, dispersive and repulsive interactions of the sample with the matrix atoms. The popularly used matrix gases Argon or Nitrogen cause only small perturbations (<1%) in the infrared features from the gas phase values for small molecules.

2.5 Multiple Trapping sites

Generally, a sample molecule is being trapped in an interstitial or substitutional site of the matrix atom. For forming the substitutional site, More than one matrix atom may be removed depending on the size of the sample molecules. Solute molecules may be trapped in sites with distinctly different environments and this causes the spectra of the trapped species to be perturbed differently depending on the environment of the site in which they are trapped, thereby resulting in multiple spectral features. And in some cases, the multiplet spectral features are not resolved and may lead to the broadening of the sample peak. Sometimes, the multiplet peak due to site effect may vanish on annealing the matrix at elevated temperatures, as the trapped species may move from the unstable site to the stable site. And the deposition rate also influences the appearance of the multiplets. Multiplet caused by the site effect can be confirmed by varying the matrix.

2.6 Aggregation

As the concentration of solute is increased, the matrix to solute ratio will decrease and molecular aggregates such as dimers, trimers and other multimers can be generated along with the monomers. A systematic concentration dependence study can be performed to identify the features due to molecular aggregates.

2.7 Molecular rotation

When small molecules are trapped in an inert matrix cage, rotations have been observed and additional spectral features will be seen, which can be identified by a temperature cycling experiment. These features due to rotation will have reversible intensity changes when a temperature cycling is carried out. However, the multiplets due to site effects do not generally show temperature cycling which sets them apart from multiplets due to rotations.

2.8 Basis Requirement of Matrix Isolation Experiments

The matrix isolation set up consists of:

1) Vacuum system- to house the cold tip where the sample is deposited.
2) Cryostat to produce the low temperatures.
3) Sample handling system with deposition lines.
4) Spectrometer to record the spectra of matrix isolated species.

The spectrometer was operated at a resolution of 1cm^{-1} and typically 8 scans were coadded to obtain good signal-to-noise ratio. All the spectra were recorded in the region 4000-400 cm^{-1}.

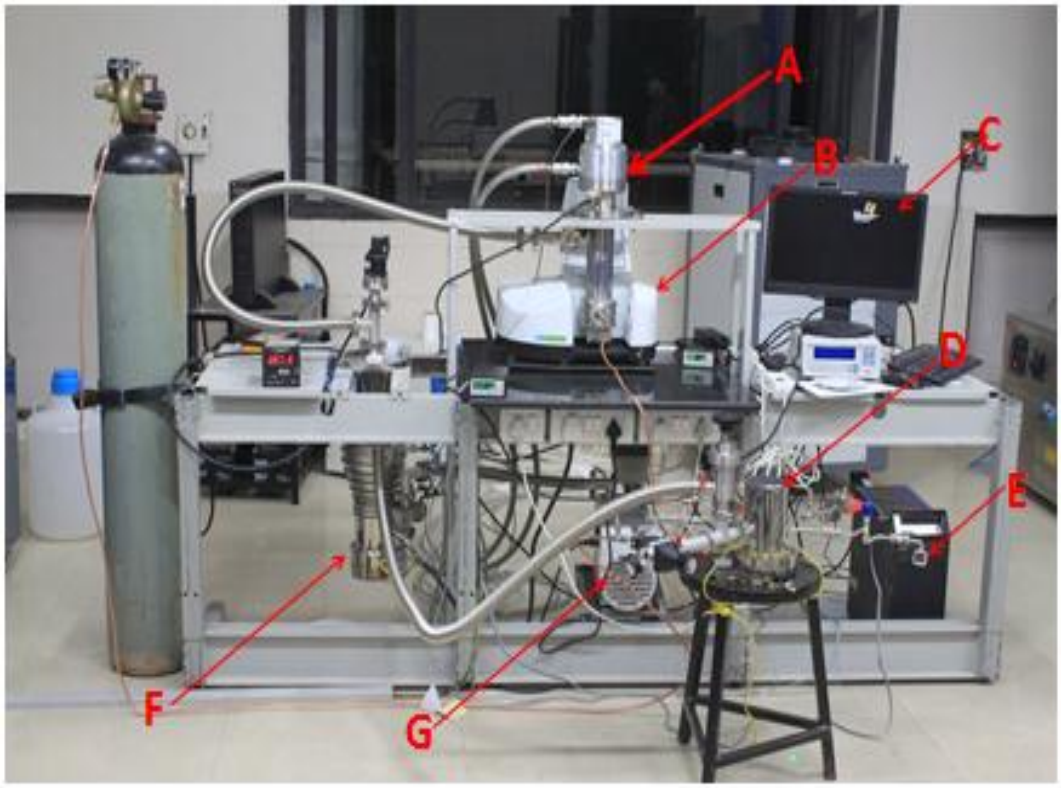

Figure 2 - Photograph of the Matrix Isolation IR spectroscopy set-up. (A) Cryostat; (B) FTIR spectrometer; (C) Data acquisition system; (D) Mixing Chamber; (E) Sample Container; (F) Diffusion pump; (G) Rotary pump.

2.9 Experimental Procedure

The sample bulb was thoroughly degassed prior to sample loading. The sample was then loaded into the bulb and subjected to several freeze-pump-thaw cycles before deposition. The samples were equilibrated at the required temperature, for about an hour, to obtain the desired vapour pressure over the sample. The temperature of the bath was measured using a platinum resistance thermometer. The desired matrix/sample ratios were thus obtained by controlling the vapour pressure over the sample. A stainless steel mixing chamber of one litre capacity was used to prepare matrix/sample gas mixtures. The mixture was then allowed to deposit on the cold KBr substrate. Rate of deposition was controlled using a fine needle valve.

Once the sample and the matrix gas are deposited at 12 K, the spectrum of the matrix isolated sample is recorded. After recording the spectrum, the temperature is raised to 30 K and the matrix is held at this temperature for about 30 minutes to an hour using the heater-temperature controller unit. The matrix is then cooled to 12 K and the spectrum is again recorded. This process called annealing is generally done to drive a reaction and also to remove the unstable sites in the matrix.

2.10 Theoretical procedure

To support the experimental work on the hydrogen bonded complexes, computations were carried out using ab initio calculations. Computations were done using Gaussian 09 package [29] to obtain the molecular properties such as structures, energies, atomic charges on the various atoms and vibrational frequencies. AIM [30] package was used to examine the nature of the interactions in the complexes.

2.10.1 Geometry Optimization of the Structure

A structure corresponding to a minimum on the potential surface is obtained using geometry optimization, which begins at molecular structure provided as input, and steps along the potential energy surface. The energy and gradient are first computed at the

point on the potential surface corresponding to the initial geometry. This information is used to determine how far and in which direction the next step is taken to improve the geometry. At the minimum (that is a stationary point), forces will be zero.

All calculations were done using a 6-311++G** basis set. Optimization was carried out at the M06, Moller-Plesset second order perturbation method (MP2), and the hybrid Hartree-Fock density functional method (B3LYP) level of theory to locate structures corresponding to minima on the potential surface. To arrive at the structures of the complexes, the geometries of monomers were first optimized; these structures were then used for the optimization of the propargyl alcohol-water complexes.

2.10.2 Stabilization energy of the complex

The stabilization energy of the complex (ΔE) is given by

$$\Delta E = E_{AB} - E_A - E_B \qquad (2)$$

; E_A, E_B and E_{AB} represent the computed energies for each species A, B, and AB respectively.

If the value of ΔE is negative, then the complex is more stable relative to the precursors. The stabilization energy of the complex was corrected for the Zero point energy (ZPE) and Basis set Superposition Error (BSSE).[31-33] We have reported the raw stabilization energies (energies not corrected for ZPE and BSSE), ZPE corrected and the BSSE corrected energies for all the complexes described in this thesis.

2.10.3 Vibrational Frequency of the complex

Frequency calculations were performed for all the complexes corresponding to the optimized geometries. It was ensured that all the frequencies were positive, that is optimization procedure did indeed correspond to a minimum. Only those structures which correspond to minima are reported. The vibrational frequency calculations also helped to assign the spectral features observed in matrix isolation experiments.

2.10.4 Atoms in molecules (AIM) analysis

Atoms-in-molecules theory was first proposed by Bader, which attempts to characterize the bonding of a system based on the topology of the electron density $[\rho(\vec{r})]$.[34,35] The wavefunctions corresponding to the optimized geometry of a molecule or complex, generated using the Gaussian package, were used as the input to generate the electron density topology. From the electron density plots, bond critical points, charge density ρ, and the Laplacian of charge density were obtained. Charge density has a definite value at each point in space. It is a scalar field defined over three dimensional space. Each topological feature of charge density has associated with it a point in space called a critical point, where the gradient of the electron density is zero $[\vec{\nabla}\rho = \vec{0}]$. Critical points are classified according to their rank and signature (λ, σ). The rank (λ) is the number of non-zero eigenvalues of the Hessian matrix of the critical point. The signature (σ) is the sum of the signs of the eigenvalues. A (3,-1) bond critical point has two negative and one positive eigenvalues and is a saddle point in the electron density.[36] If a (3,-1) bond critical point is found between the XH and π moieties then generally a hydrogen bond is considered to be present.[37]

Non-covalent interactions (NCI) index is a complementary approach to AIM theory that is also based on the electron density and its gradients and can be used to characterize both attractive and repulsive intermolecular interactions.[38] The NCI index is constructed from the reduced density gradient, s, and the electron density, ρ, where,

$$s = \frac{1}{2(3\pi^2)^{1/3}} \frac{|\vec{\nabla}\rho|}{\rho^{4/3}} \qquad \text{.....(3)}$$

Weak inter- or intramolecular interactions correspond to troughs in s(ρ). These troughs can be characterized by the sign of the second eigenvalue, λ_2, which is negative for attractive interactions such as hydrogen bonding and positive for repulsive interactions.[38]

CHAPTER 3
PROPARGYL ALCOHOL MONOMER AND ITS DIMER

3.1 Introduction

Due to internal rotation of the C-OH group, propargyl alcohol can exist in two forms: the gauche form and trans form with respect to the carbon chain of the molecule.[24]

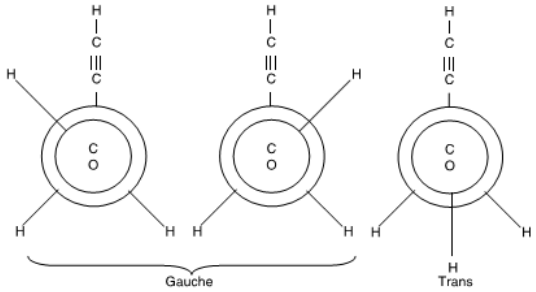

Figure 3- Conformers of propargyl alcohol[6]

Propargyl alcohol can be derived from methyl alcohol by substitution of one methyl hydrogen with an acetylenic group.

Propargyl alcohol is an excellent candidate for interstellar detection and potentially a good probe of the relative importance of gas phase ion driven chemical processes or dust grain surface driven chemical processes, thus is observable in both warm and cold interstellar regions. The structural isomer of PA, propenal has been detected in the interstellar medium [39]. The prospects for interstellar detection are greatly enhanced due to the tunnelling between the gauche+ and gauche- substates, which enables propargyl alcohol to exhibit a strong submillimeter spectrum even at low temperatures.[6]

In combustion chemistry, combination of two propargyl radicals is considered to be an important channel for the formation of benzene, that is a route to the formation of polycyclic aromatic hydrocarbons (PAHs) and thus soot formation [Eq. (4) :[40,41]

$$C_3H_3 + C_3H_3 \rightarrow C_6H_6 \rightarrow PAH \rightarrow soot \quad \ldots\ldots\ldots (4)$$

In a shock-tube study, by Tranter et al., the kinetics of this reaction has been investigated.[42] The intermolecular potentials control the chemical reactions and the first

step to the potential is the equilibrium structure of molecular complexes. In this study, we have examined the nature of H-bonds between propargyl alcohol and water.

In experiments on the hydrogen bonded complexes of propargyl alcohol with water (discussed in chapter 4), it was necessary to study the spectra of propargyl alcohol monomer in argon and nitrogen matrices. This chapter gives a detailed account on the spectroscopy of propargyl alcohol in argon and nitrogen matrices.

The study of propargyl alcohol dimer has received considerable attention. Arunan's group have recorded a pure rotational spectrum of propargyl alcohol dimer [43]. There is a need for experiments on propargyl alcohol dimer in both solid Ar and N_2 and a comparison with the computations. This chapter presents data on the propargyl alcohol dimer in argon and nitrogen matrices. Experimental frequencies in the two matrices were corroborated with the computed vibrational frequencies.

3.2 Experimental

Most of the experimental details have already been discussed in chapter 2. Only aspects of the experiments relevant to the propargyl alcohol and its dimer will be discussed in this chapter. Both argon and nitrogen matrices were used for the matrix isolation experiments for the propargyl alcohol and its dimer. Propargyl alcohol was first subjected to several freeze-pump-thaw cycles. Propargyl alcohol and the matrix gases, argon or nitrogen, were mixed in the desired ratios. In our experiments, matrix to propargyl alcohol ratios ranging from 1500:1 to 70:1 were used.

3.3 Results and discussion

3.3.1 Propargyl alcohol monomer in nitrogen and argon matrices

Figure 4 and Figure 5 shows the matrix isolation IR spectra of propargyl alcohol in nitrogen and argon matrix respectively. The region spanned in this figure is that between 3750-3400 cm^{-1} and 1070-1000 cm^{-1}.

In the N_2 matrix, propargyl alcohol has absorptions at 3641.64, 3310.08, and 1040.12 cm^{-1} for O-H stretch, C-H acetylenic stretch, and the C-O stretch respectively.

In the argon matrix, propargyl alcohol has absorptions at 3649.41, (3319.86, 3317.01), 1042.54 cm^{-1} for O-H stretch, C-H acetylenic stretch, and the C-O stretch respectively. Propargyl alcohol has strong absorptions at 3319.86 and 3317.01 cm^{-1}. The corresponding feature in the nitrogen matrix, appear as a strong feature at 3310.08 cm^{-1}.

Clearly, the spectrum of propargyl alcohol in nitrogen shows marked differences from that observed in the argon matrix. First the O-H stretch for propargyl alcohol in the N_2 matrix occur at 7.8 cm^{-1} to the blue compared with its position in the Ar matrix, while the C-H acetylenic stretch is blue shifted and the C-O stretch is blue shifted by 2.4 cm^{-1} , indicating a small perturbation of the propargyl alcohol, by the different matrices. Secondly, there is a doublet seen in the Ar matrix at 3319.86 and 3317.01 cm^{-1}.

In literature on the study of classical and quantum dynamics of overtone excitations, it has been reported that in propargyl alcohol, an accidental degeneracy occurs between the overtone state and a combination state and intensity sharing occurs, thus both states appear with nearly equal intensity in the spectrum. In the $\Delta v_{OH} = 5$ OH stretching overtone region, a shoulder is seen emerging from low energy side of main OH-stretching band, due to weak resonance with a combination band between $\Delta v_{OH} = 4 + \Delta v_{CH} = 1$. The dark state has no intrinsic intensity so borrows intensity from $\Delta v_{OH} = 5$ transition.[22]

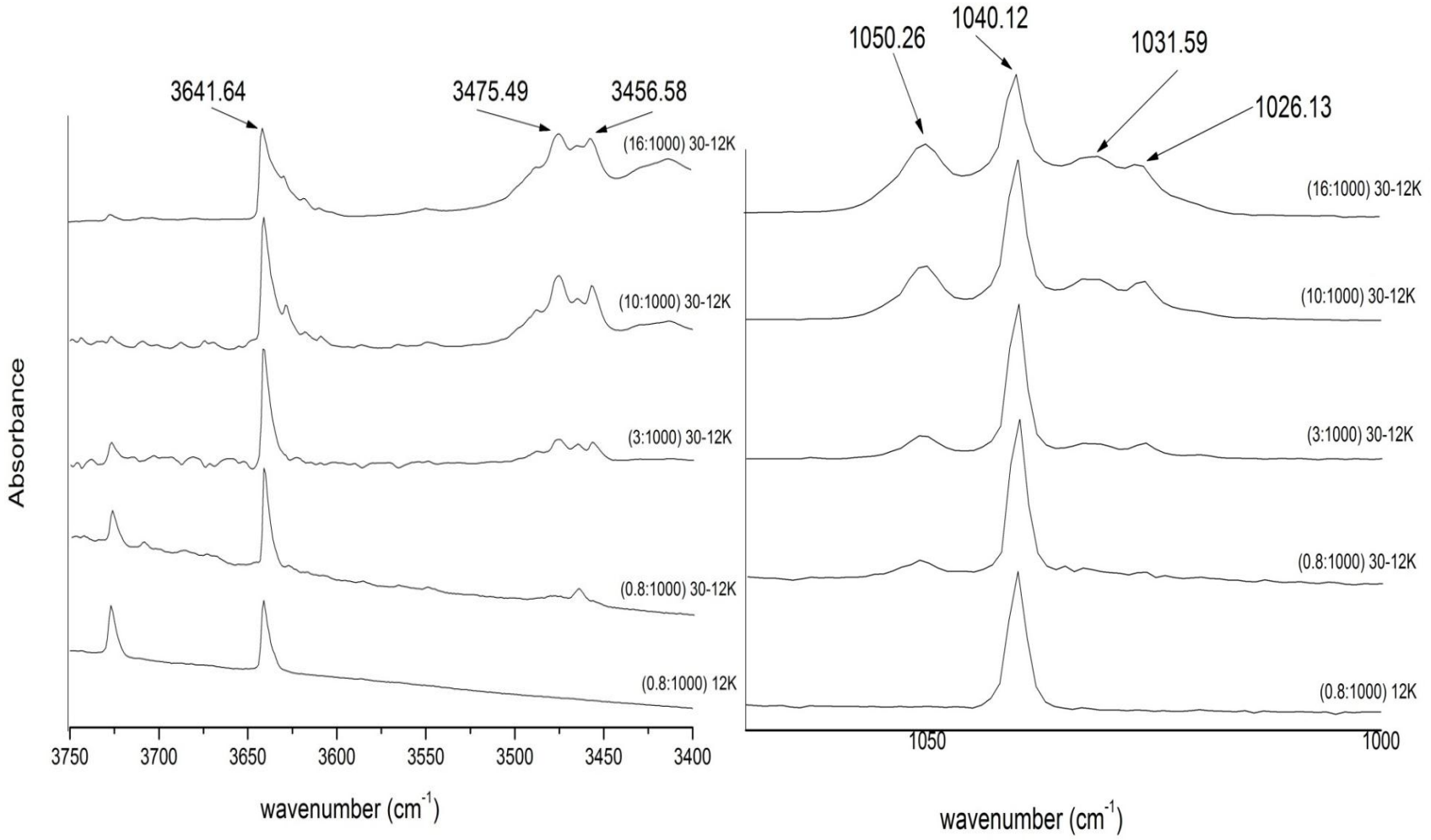

Figure 4- IR spectrum of propargyl alcohol in N_2 matrix in the region 3750-3400 cm^{-1} and 1070-1000 cm^{-1}

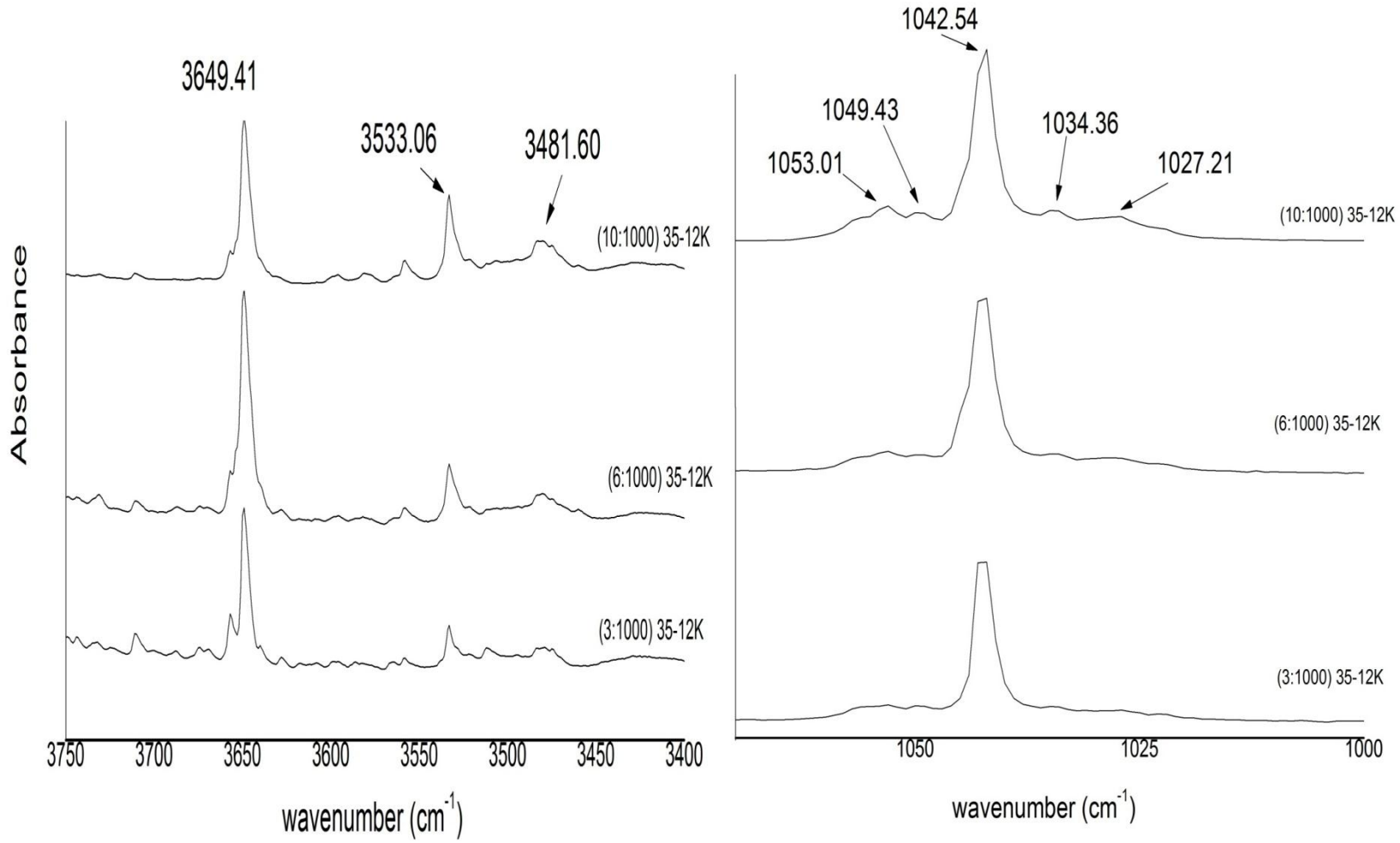

Figure 5- IR spectrum of propargyl alcohol in Ar matrix in the region 3750-3400 cm^{-1} and 1070-1000 cm^{-1}

Propargyl Alcohol (PA) has two stable conformers, shown in Fig. 3. The gauche form is lower in energy than the trans form by 1.6 kcal/mol calculated at the CCSD(T)-F12/VDZ-F12 level of theory [1] .

We performed calculations on propargyl alcohol using three different levels of theroy M06, MP2 and B3LYP for the calculation of the propargyl alcohol monomer, using a 6-311++G** basis set. The optimized geometries obtained at each of the above levels of calculations are shown in **Figure 6**.

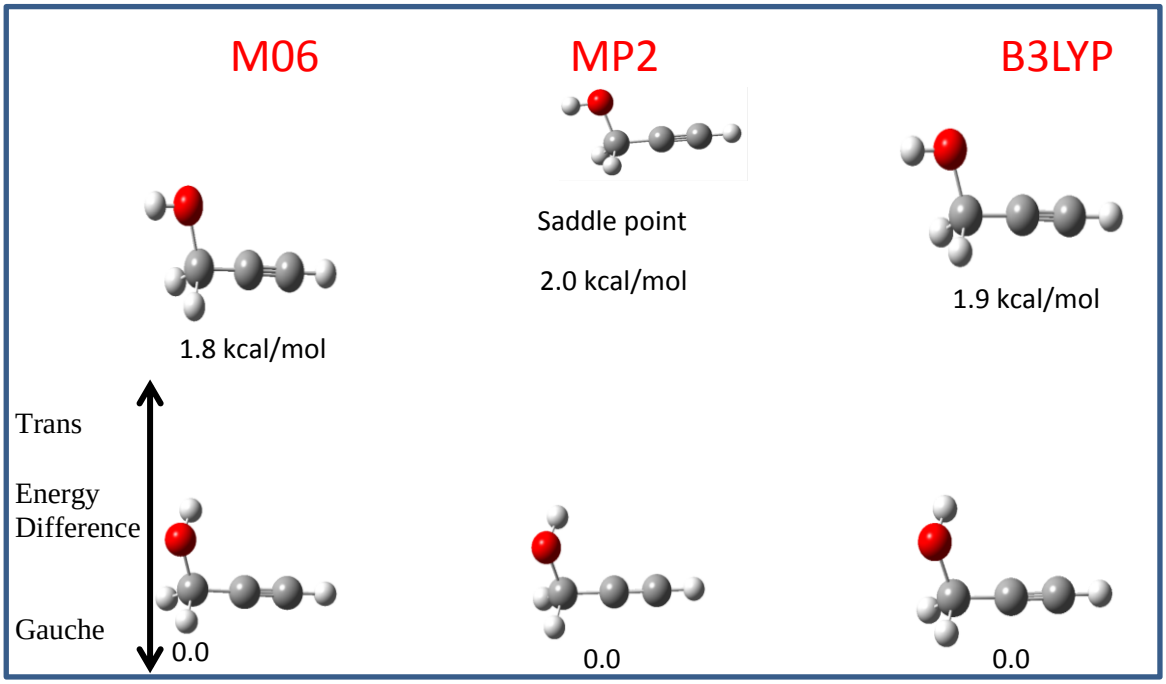

Figure 6 - Optimized geometries of propargyl alcohol monomer at various levels of theory

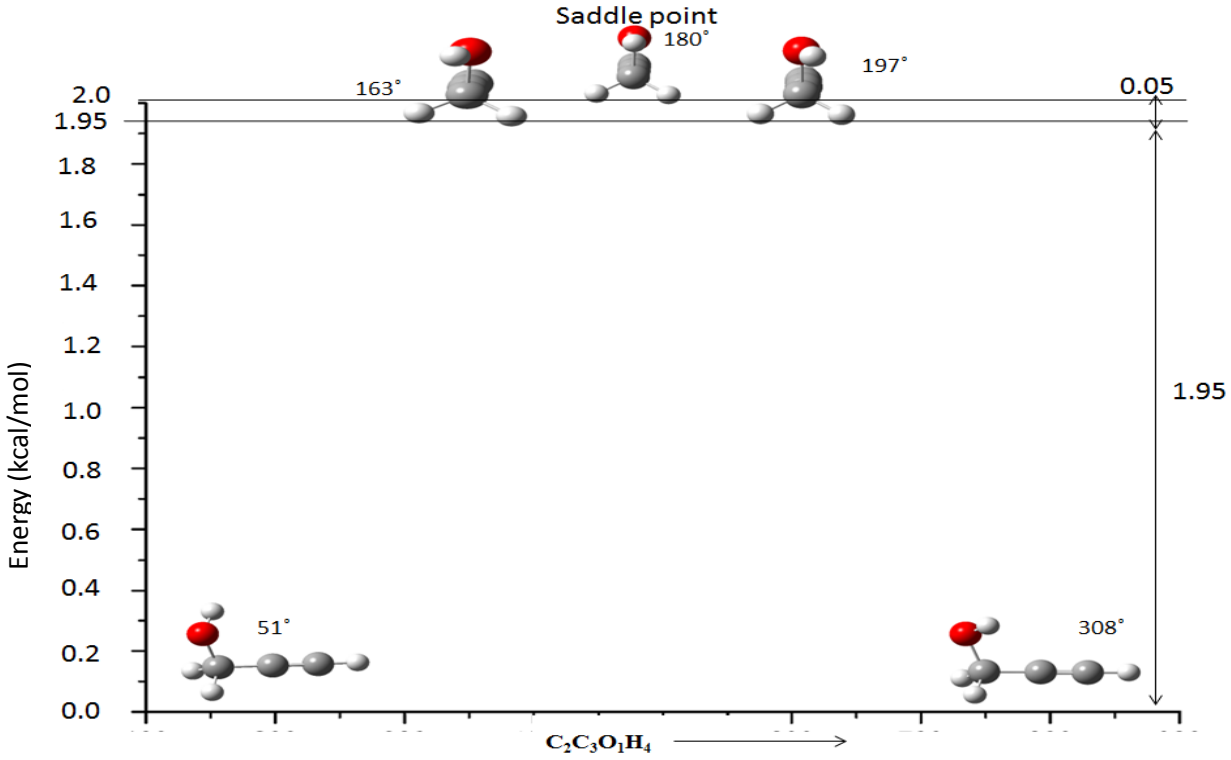

Figure 7- Propargyl Alcohol molecule as a function of the dihedral angle ($C_2C_3O_1H_4$) at the MP2/6-311+G(d,p) level of theory.

The trans form, with a $C_2C_3O_1H_4$ dihedral angle exactly 180°, is a saddle point at this level of calculation and separates two equivalent minima with $C_2C_3O_1H_4$ dihedral angles of 163° and 197°. However, the energy barrier for interconversion of these two equivalent forms is 0.05 kcal mol^{-1}.

3.3.2 Propargyl alcohol dimer in the nitrogen and argon matrices

Figure 4 and Figure 5 shows the spectra of propargyl alcohol in nitrogen and argon matrices. When propargyl alcohol was deposited in Ar and N_2 matrix and the matrix then annealed at 30 K, new features appear at 3475.49, 3456.58, 1050.26, 1032.87, 1031.13, 1026.13 cm^{-1} in N_2 (Figure 4) and 3533.06, 3481.60, 1053.01, 1049.43, 1034.36, 1027.21 cm^{-1} in Ar (Figure 5). Furthermore, these bands increased in intensity as the concentration of propargyl alcohol was increased, indicating that they belong to the propargyl alcohol dimer.

3.4 Structure of the propargyl alcohol dimer

Table 1- Optimized geometries and AIM analysis of propargyl alcohol dimer at various levels of theory (*Red sphere =O atom, Black sphere=C atom and Grey sphere= H atom in AIM*)

	M06	**MP2**	**B3LYP**
Dimer	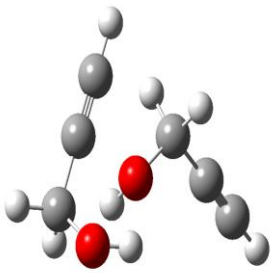	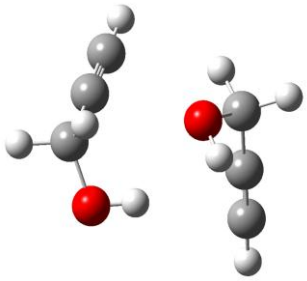	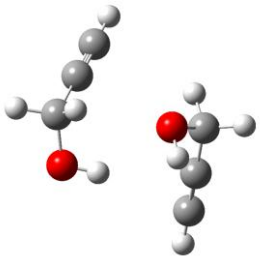

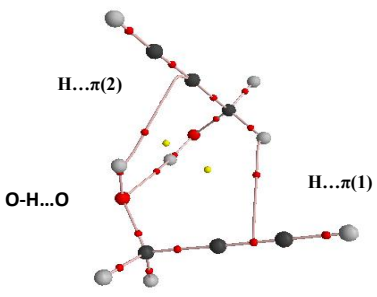

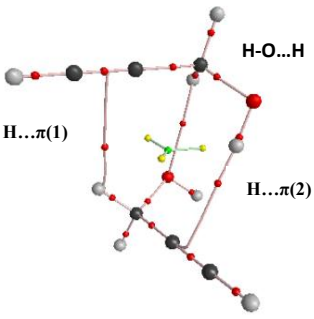

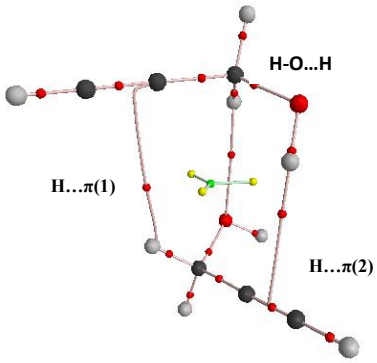

At M06	ρ (r) in a.u.	$\nabla^2\rho(r)$ in a.u.
H…π(1)	0.0059	-0.0041
H…π(2)	0.0124	-0.0104
O-H…O	0.0232	-0.0239
At MP2	ρ (r) in a.u.	$\nabla^2\rho(r)$ in a.u.
H…π(1)	0.0059	-0.0041
H…π(2)	0.0104	-0.0085
H-O…H	0.0082	-0.0073
At B3LYP	ρ (r) in a.u.	$\nabla^2\rho(r)$ in a.u.
H… π(1)	0.0031	-0.0022
H… π(2)	0.0087	-0.0068
H-O…H	0.0065	-0.0055

It has been reported that propargyl alcohol dimer structure have been optimized at the MP2 level of theory using 6-311+G(3df,2p) basis set.[43] In our experiment we observed that Experimental features obtained corresponds to the computed M06 dimer structure.

3.5 AIM Analysis

The Electron density topology of the dimer was examined using the AIMPAC package.

3.6 Vibrational Assignments

Table 2, 3, 4 gives the computed frequencies and their intensities (in brackets) for the propargyl alcohol dimer optimized at M06, MP2, B3LYP levels of theory using 6-311++G(d,p) basis set. The computed vibrational frequencies were scaled for the purpose of comparison with experimental results.

The computed shifts for dimer were obtained by subtracting computed vibrational frequency of dimer from computed vibrational frequency of monomer for each normal mode.

Table 2- Computed and scaled frequencies of the propargyl alcohol dimer at M06/6-311++G (d, p)

M06/6-311++ G(d,p) in Nitrogen matrix		
Computed ν	Scaled ν	Mode of assignment
3778.97(372)	3535.23	Coupled O_{15}-H_{16} O_7-H_8 antisym.
3752.72(103)	3510.67	Coupled O_{15}-H_{16} O_7-H_8 sym.
3443.49(53)	3302.65	C_{10}-H_{11}(acetylenic)
3442.36(57)	3301.57	C_2-H_3(acetylenic)
1116.74(119)	1056.77	C_{12}-O_{15} stretch
1091.74(131)	1033.11	C_4-O_7 stretch
M06/6-311++ G(d,p) in Argon matrix		
Computed ν	Scaled ν	Mode of assignment
3778.97(372)	3542.78	Coupled O_{15}-H_{16} O_7-H_8 antisym.
3752.72(103)	3518.17	Coupled O_{15}-H_{16} O_7-H_8 sym.
3443.49(53)	3309.54	C_{10}-H_{11}(acetylenic)
3442.36(57)	3308.45	C_2-H_3(acetylenic)
1116.74(119)	1059.23	C_{12}-O_{15} stretch
1091.74(131)	1035.51	C_4-O_7 stretch

Table 3- Computed and scaled frequencies of the propargyl alcohol dimer at MP2/6-311++G (d, p)

MP2/6-311++ G(d,p) in Nitrogen matrix		
Computed ν	Scaled ν	Mode of assignment
3872.05(43)	3629.27	O_{15}-H_{16}
3846.36(166)	3605.19	O_7-H_8
3500.06(52)	3308.26	C_2-H_3 (acetylenic)
3494.75(64)	3303.24	C_{10}-H_{11}(acetylenic)
1085.08(93)	1041.46	C_4-O_7 stretch
1073.77(88)	1030.60	C_{12}-O_{15} stretch
MP2/6-311++ G(d,p) in Argon matrix		
Computed ν	Scaled ν	Mode of assignment
3872.05(43)	3637.02	O_{15}-H_{16}
3846.36(166)	3612.89	O_7-H_8
3500.06(52)	3315.26	C_2-H_3 (acetylenic)
3494.75(64)	3310.23	C_{10}-H_{11}(acetylenic)
1085.08(93)	1043.85	C_4-O_7 stretch
1073.77(88)	1032.97	C_{12}-O_{15} stretch

Table 4- Computed and scaled frequencies of the propargyl alcohol dimer at B3LYP/6-311++G (d, p)

B3LYP/6-311++ G(d,p) in Nitrogen matrix		
Computed ν	Scaled ν	Mode of assignment
3823.41(40)	3636.06	O_{15}-H_{16}
3773.65(177)	3588.74	O_7-H_8
3474.59(59)	3310.24	C_2-H_3 (acetylenic)
3469.33(70)	3305.23	C_{10}-H_{11} (acetylenic)
1045.83(101)	1041.44	C_4-O_7
1038.73(83)	1034.37	C_{12}-O_{15}
B3LYP/6-311++ G(d,p) in Argon matrix		
Computed ν	Scaled ν	Mode of assignment
3823.41(40)	3644.09	O_{15}-H_{16}
3773.65(177)	3596.67	O_7-H_8
3474.59(59)	3317.19	C_2-H_3 (acetylenic)
3469.33(70)	3312.17	C_{10}-H_{11} (acetylenic)
1045.83(101)	1043.84	C_4-O_7
1038.73(83)	1036.76	C_{12}-O_{15}

3.7 Conclusions

The features of propargyl alcohol in argon and nitrogen matrix have been assigned experimentally. The formation of the propargyl alcohol dimer was evidenced by appearance of new peaks on increasing the concentration of propargyl alcohol. Ab initio computations are performed to rationalize the experimental observation at M06, MP2 and B3LYP levels using 6-311++G** basis set. Vibrational frequency calculation on the dimer helped us to assign the experimentally observed features.

It was observed that optimized structure obtained at M06 has been seen experimentally as for coupled O_{15}-H_{16} O_7-H_8 antisym. Mode, Computed shift was +106 and for Coupled O_{15}-H_{16} O_7-H_8 sym. Computed shift was +131, however the experimental shift was +166 and +185, respectively in the N_2 matrix. However, for coupled O_{15}-H_{16} O_7-H_8 antisym. Mode, Computed shift was +107 and for Coupled O_{15}-H_{16} O_7-H_8 sym. Computed shift was +131 , however the experimental shift was +116 and +168, respectively in the Ar matrix.

Similarly, for C_{12}-O_{15} stretch Mode, Computed shift was -17 and for C_4-O_7 stretch Computed shift was +7, however the experimental shift was -10 and +8, respectively in the N_2 matrix. However, for C_{12}-O_{15} stretch Mode, Computed shift was -17 and for C_4-O_7 stretch Computed shift was +7, however the experimental shift was -10 and +8, respectively in the Ar matrix.

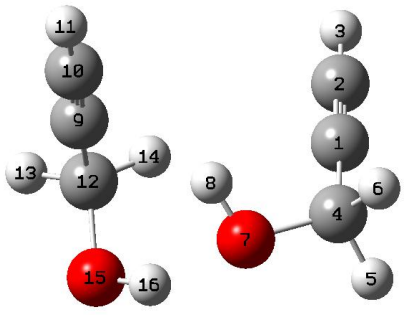

CHAPTER 4

PROPARGYL ALCOHOL AND WATER HYDROGEN BONDED COMPLEXES

==========

4.1 Introduction

As propargyl alcohol has multiple sites for hydrogen bonding interaction, and further given the fact that propargyl alcohol exists in two different conformations, multiple minima can be expected on the potential surface. In order to investigate the relative preference for these hydrogen bonding sites, the complexes of propargyl alcohol and water were studied.

4.2 Experimental

Most of the experimental details have already been discussed in chapter 2. Both argon and nitrogen matrices were used for the matrix isolation experiments for the complexes of propargyl alcohol with water. Propargyl alcohol and millipore water were first subjected to several freeze-pump-thaw cycles. Propargyl alcohol, water and the matrix gases, argon or nitrogen were mixed in the desired ratios.

4.3 Computational details

The computational study was performed using the GAUSSIAN 09 suite of programmes. The equilibrium geometries and vibrational frequencies were calculated using the B3LYP and Minnesota functional M06 and second order Moller-Plesset perturbation theory (MP2) with a 6-311++G(d,p) basis set. The stabilization energies were calculated at each of these levels of theory, as follows:

$\Delta E = E_{AB} - (E_A + E_B)$

$\Delta E_{BSSE} = E_{AB}(AB) - \{E_A(AB) + E_B(AB)\}$,

where E_A , E_B and E_{AB} represent the computed energies for each species A,B and AB respectively.

Stabilization energies were also individually corrected for the zero point energy (ZPE) and the basis set superposition errors (BSSE). BSSE correction was implemented using the counterpoise (CP) scheme of Boys and Bernadi. [44] The frequency calculations were performed at all the levels of theories mentioned above to ensure that the optimized geometries were indeed a minimum on the potential surface and also to aid us in assigning the features observed in the experiments. Using the computed experimental frequencies, the infrared spectrum of the complexes and the monomers were also simulated using Gauss-View assuming a line width of 1 cm^{-1}. Atoms in Molecule theory was performed to identify the critical points in the complexes to understand the bonding features.

4.4 Results and discussions

When propargyl alcohol and water were codeposited, product absorption band appeared at 3465.23 and 1050.97 cm^{-1} in the N_2 matrix and at 3512.09 and 1055.96 cm^{-1} in the Ar matrix. These bands appeared only when both the reagents were codeposited. Also, with the increase in concentration of either of the two reagents, these bands increased in intensity. These observations clearly indicate that these features are due to a complex involving propargyl alcohol and water. It was observed that the experimental shift for the O-H stretch of PA was +176 and for the C-O stretch was -11, respectively in N_2 matrix. Similarly the experimental shift for the O-H stretch of PA was +137 and for the C-O stretch was -13, respectively in Ar matrix.

Table 5 – Optimized geometries of the different propargyl alcohol-water complexes at various levels of theory

Complexes	M06	MP2	B3LYP
Complex 1	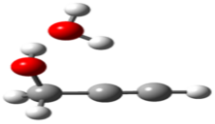	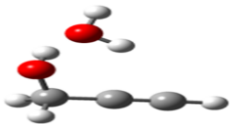	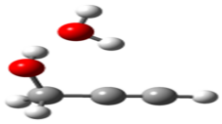
Complex 2	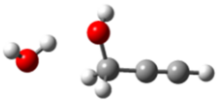	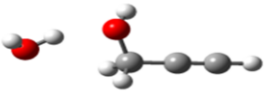	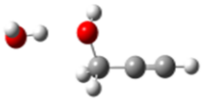
Complex 3	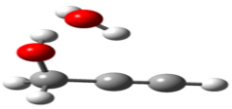	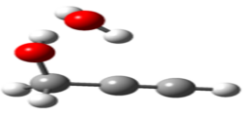	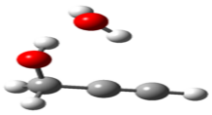
Complex 4	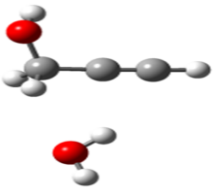	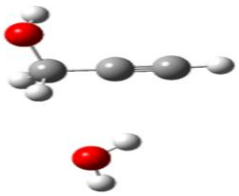	
Complex 5	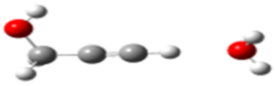	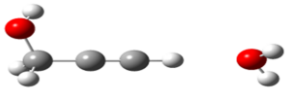	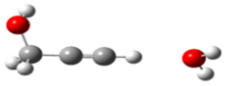
Complex 6	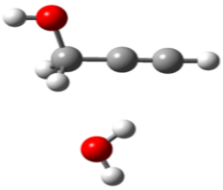	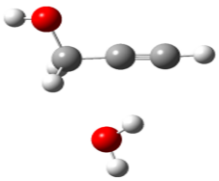	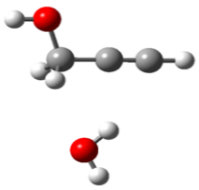
Complex 7	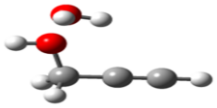	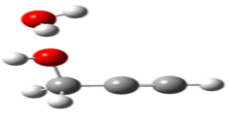	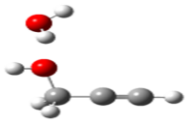
Complex 8	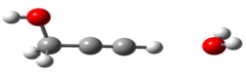	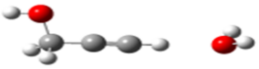	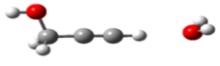
Complex 9	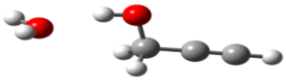	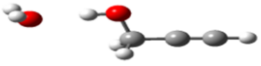	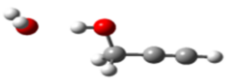

Table 6 – Computed stabilization energy of the complexes at M06/6-311++G (d, p)

Stabilization Energy at M06/6-311++G (d, p)			
Complex	$\Delta E_{RAW}/\Delta E_{ZPE}/\Delta E_{BSSE}$ (kcal/mol)	Complex	$\Delta E_{RAW}/\Delta E_{ZPE}/\Delta E_{BSSE}$ (kcal/mol)
Complex 1	-8.5/-6.5/-7.6	Complex 6	-3.9/-2.5/-3.6
Complex 2	-6.1/-4.2/-5.5	Complex 7	-6.6/-4.3/-5.9
Complex 3	-8.4/-6.4/-7.5	Complex 8	-3.4/-2.2/-2.6
Complex 4	-3.6/-2.0/-3.2	Complex 9	-7.1/-5.4/-6.1
Complex 5	-3.7/-2.3/-3.0		

Table 7 – Computed stabilization energy of the complexes at MP2/6-311++G (d, p)

Stabilization Energy at MP2/6-311++G (d, p)			
Complex	$\Delta E_{RAW}/\Delta E_{ZPE}/\Delta E_{BSSE}$ (kcal/mol)	Complex	$\Delta E_{RAW}/\Delta E_{ZPE}/\Delta E_{BSSE}$ (kcal/mol)
Complex 1	-4.8/-2.8/-2.4	Complex 6	-1.6/+0.1/-0.4
Complex 2	-3.9/-2.1/-2.4	Complex 7	-4.1/-1.7/-2.2
Complex 3	-4.5/-2.6/-2.2	Complex 8	-2.4/-0.2/-0.9
Complex 4	-1.3/-0.4/-0.1	Complex 9	-5.4/-3.4/-3.4
Complex 5	-2.8/-1.1/-1.3		

Table 8 – Computed stabilization energy of the complexes at B3LYP/6-311++G (d, p)

Stabilization Energy at B3LYP/6-311++G (d, p)			
Complex	$\Delta E_{RAW}/\Delta E_{ZPE}/\Delta E_{BSSE}$ (kcal/mol)	Complex	$\Delta E_{RAW}/\Delta E_{ZPE}/\Delta E_{BSSE}$ (kcal/mol)
Complex 1	-6.6/-4.5/-5.8	Complex 6	-2.6/-1.5/-2.3
Complex 2	-5.4/-3.6/-4.8	Complex 7	-5.6/-3.5/-4.9
Complex 3	-6.3/-4.3/-5.6	Complex 8	-3.1/-1.7/-2.4
Complex 5	-3.3/-2.0/-2.6	Complex 9	-6.4/-4.6/-5.4

At all the levels of theory (M06, MP2 and B3LYP) Complex 1 and complex 3, which differ only in the orientation of the water molecule turned out to be most stable hydrogen bonded complexes of propargyl alcohol with water.

Figure 6 and Figure 7 shows the matrix isolation IR spectra of propargyl alcohol with water in nitrogen and argon matrix respectively. The region spanned in this figure is that between 3750-3400 cm^{-1} and 1070-1000 cm^{-1} (for N_2 matrix) and between 3850-3400 cm^{-1} and 1070-1000 cm^{-1} (for Ar matrix).

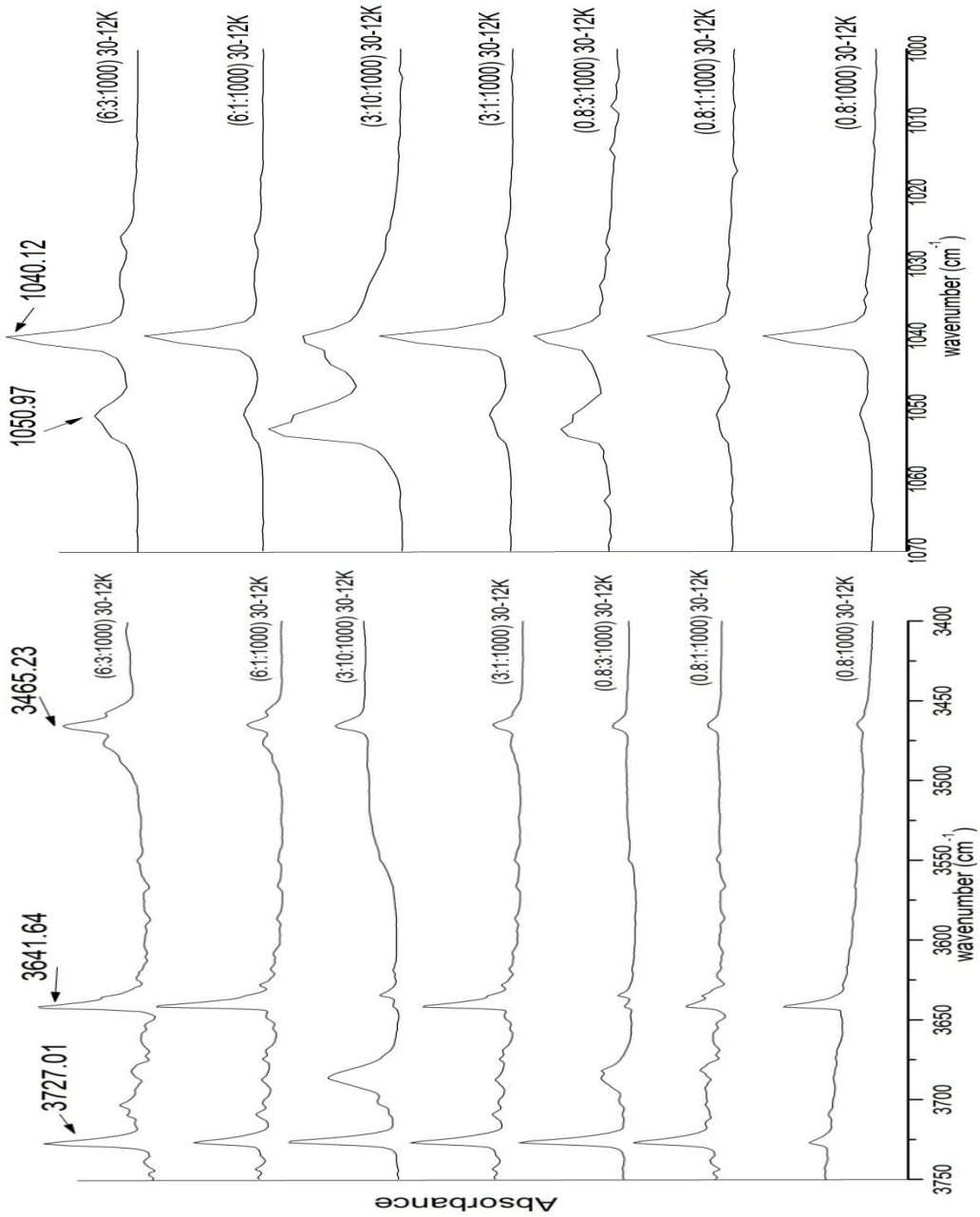

Figure 8-IR spectrum of propargyl alcohol with water in Nitrogen matrix in the region 3750-3400 cm^{-1} and 1070-1000 cm^{-1}

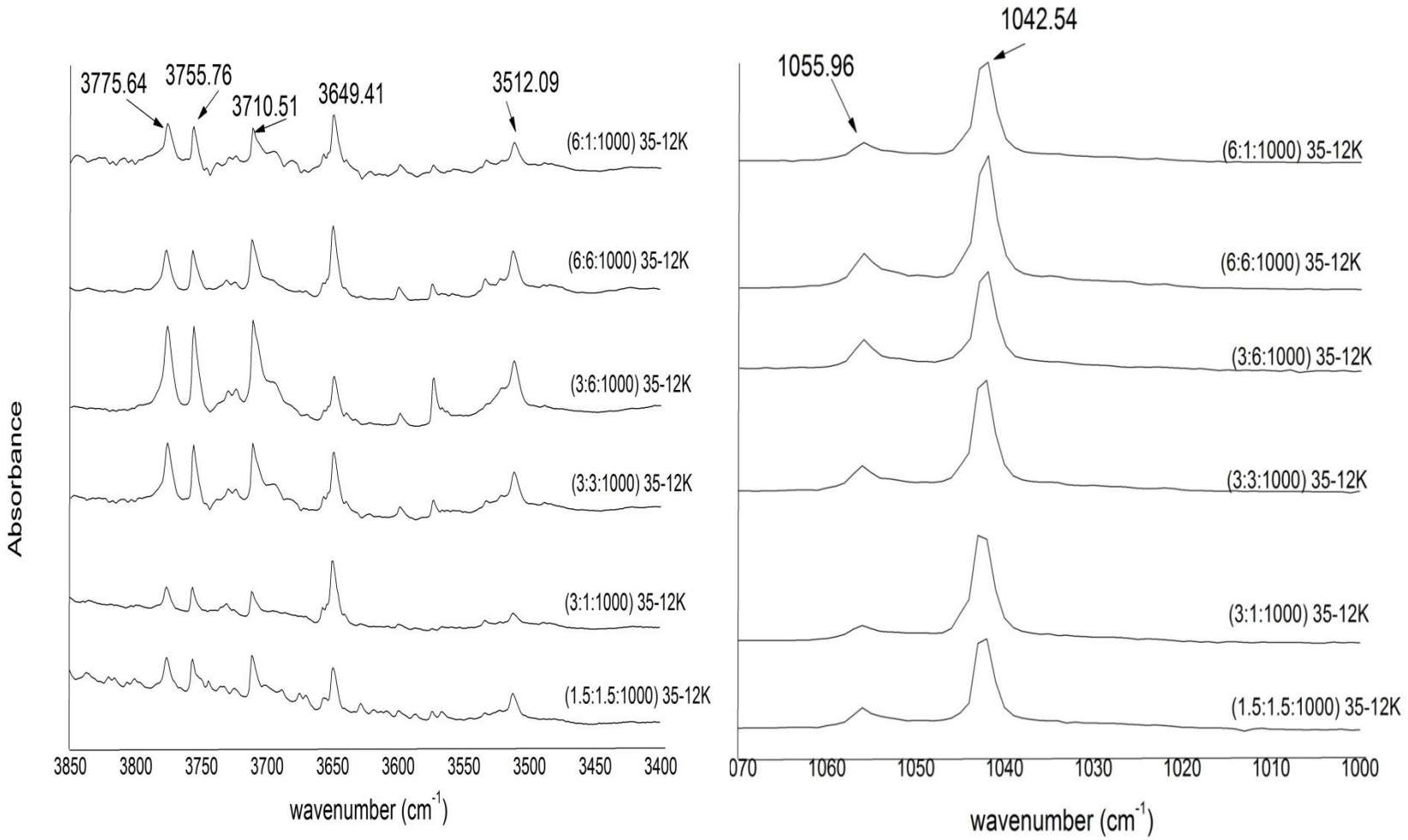

Figure 9- IR spectrum of propargyl alcohol with water in Argon matrix in the region 3950-3400 cm^{-1} and 1070-1000 cm^{-1}

Table 9 –Computed and scaled frequencies of the monomers (gauche PA and water) and the complexes at M06/6-311++G (d, p) in N_2 matrix

	Computed ν	Scaled ν	Exp. ν	Scaled Shifts ($\nu_{complex}$ - $\nu_{monomer}$)	Mode of Assignment
Monomer	3892.77(52)	3641.69	3641.64		O-H stretch PA
	3451.24(50)	3310.08	3310.08		C-H acetylenic stretch
	1099.13(131)	1040.11	1040.12		C-O stretch
	4015.19(84)	3726.90	3727.01		O-H asym. H_2O
	3891.78(17)	3634.14	3634.20		O-H sym. H_2O
Complex 1	3716.27(287)	3476.57	3465.23	-165	O-H stretch PA
	3446.59(52)	3305.62		-4	C-H acetylenic stretch
	1119.49(125)	1059.37	1050.97	+19	C-O stretch
	3972.97(157)	3687.71		-39	O-H asym. H_2O
	3809.17(143)	3557.00		-77	O-H sym. H_2O
Complex 2	3890.50(60)	3639.56		-2	O-H stretch PA
	3450.36(54)	3309.24		-1	C-H acetylenic stretch
	1082.05(122)	1023.94		-16	C-O stretch
	3979.99(135)	3694.23		-33	O-H asym. H_2O
	3767.37(311)	3517.97		-116	O-H sym. H_2O
Complex 3	3728.16(273)	3487.69	3465.23	-154	O-H stretch PA
	3446.24(53)	3305.29		-5	C-H acetylenic stretch
	1121.35(123)	1061.13	1050.97	+21	C-O stretch
	3973.82(154)	3688.50		-38	O-H asym. H_2O
	3810.43(147)	3558.18		-76	O-H sym. H_2O
Complex 4	3893.76(53)	3642.61		+1	O-H stretch PA
	3445.22(55)	3304.31		-6	C-H acetylenic stretch
	1103.47(135)	1044.21		+4	C-O stretch
	3982.49(144)	3696.55		-30	O-H asym. H_2O
	3833.59(88)	3579.81		-54	O-H sym. H_2O
Complex 5	3896.01(50)	3644.72		+3	O-H stretch PA
	3355.55(301)	3218.31		-91	C-H acetylenic stretch
	1095.41(129)	1036.59		-3	C-O stretch
	4004.21(105)	3716.71		-10	O-H asym. H_2O
	3883.15(28)	3626.08		-8	O-H sym. H_2O

Table 10 –Computed and scaled frequencies of the monomers (gauche PA and water) and the complexes at MP2/6-311++G (d, p) in N_2 matrix

	Computed ν	Scaled ν	Exp. ν	Scaled Shifts ($\nu_{complex}$ - $\nu_{monomer}$)	Mode of Assignment
Monomer	3885.13(41)	3641.53	3641.64		O-H stretch PA
	3502.06(55)	3310.15	3310.08		C-H acetylenic stretch
	1083.70(108)	1040.13	1040.12		C-O stretch
	4003.00(63)	3726.79	3727.01		O-H asym. H_2O
	3884.75(57)	3634.18	3634.20		O-H sym. H_2O
Complex 1	3765.13(275)	3529.06	3465.23	-112	O-H stretch PA
	3496.97(57)	3305.34		-5	C-H acetylenic stretch
	1098.79(107)	1054.62	1050.97	+14	C-O stretch
	3974.65(117)	3700.40		-26	O-H asym. H_2O
	3848.61(44)	3600.37		-34	O-H sym. H_2O
Complex 2	3878.39(47)	3635.21		-6	O-H stretch PA
	3501.12(59)	3309.26		-1	C-H acetylenic stretch
	1067.43(113)	1024.52		-16	C-O stretch
	3968.00(118)	3694.21		-33	O-H asym. H_2O
	3779.97(297)	3536.16		-98	O-H sym. H_2O
Complex 3	3774.07(246)	3537.44	3465.23	-104	O-H stretch PA
	3496.59(58)	3304.98		-5	C-H acetylenic stretch
	1100.26(106)	1056.03	1050.97	+16	C-O stretch
	3976.20(120)	3701.84		-25	O-H asym. H_2O
	3846.40(54)	3598.31		-36	O-H sym. H_2O
Complex 4	3885.84(39)	3642.20		+1	O-H stretch PA
	3497.25(58)	3305.60		-4	C-H acetylenic stretch
	1081.86(113)	1038.37		-2	C-O stretch
	3985.69(103)	3710.68		-16	O-H asym. H_2O
	3860.54(25)	3611.53		-23	O-H sym. H_2O
Complex 5	3884.92(39)	3641.33		0	O-H stretch PA
	3436.30(231)	3247.99		-62	C-H acetylenic stretch
	1080.62(109)	1037.18		-3	C-O stretch
	3990.71(79)	3715.35		-11	O-H asym. H_2O
	3874.40(18)	3624.50		-10	O-H sym. H_2O

Table 11 –Computed and scaled frequencies of the monomers (gauche PA and water) and the complexes at B3LYP/6-311++G (d, p) in N_2 matrix

	Computed ν	Scaled ν	Exp. ν	Scaled Shifts ($\nu_{complex}$ - $\nu_{monomer}$)	Mode of Assignment
Monomer	3829.16(35)	3641.53	3641.64		O-H stretch PA
	3474.56(62)	3310.21	3310.08		C-H acetylenic stretch
	1044.47(109)	1040.08	1040.12		C-O stretch
	3922.33(57)	3727.00	3727.01		O-H asym. H_2O
	3817.10(9)	3634.26	3634.20		O-H sym. H_2O
Complex 1	3666.35(306)	3486.70	3465.23	-155	O-H stretch PA
	3469.92(66)	3305.79		-4	C-H acetylenic stretch
	1061.60(111)	1057.14	1050.97	+17	C-O stretch
	3896.81(112)	3702.75		-24	O-H asym. H_2O
	3772.91(74)	3592.19		-42	O-H sym. H_2O
Complex 2	3823.42(46)	3636.07		-5	O-H stretch PA
	3473.52(67)	3309.22		-1	C-H acetylenic stretch
	1030.45(126)	1026.12		-14	C-O stretch
	3891.18(101)	3697.40		-30	O-H asym. H_2O
	3690.96(438)	3514.16		-120	O-H sym. H_2O
Complex 3	3678.04(286)	3497.82	3465.23	-144	O-H stretch PA
	3469.69(66)	3305.57		-5	C-H acetylenic stretch
	1063.40(109)	1058.93	1050.97	+19	C-O stretch
	3900.92(110)	3706.65		-20	O-H asym. H_2O
	3774.46(76)	3593.66		-41	O-H sym. H_2O
Complex 5	3828.79(33)	3641.18		0	O-H stretch PA
	3393.16(270)	3232.66		-77	C-H acetylenic stretch
	1041.31(110)	1036.94		-3	C-O stretch
	3919.55(75)	3724.36		-3	O-H asym. H_2O
	3816.72(16)	3633.90		0	O-H sym. H_2O

Table 12 –Computed and scaled frequencies of the monomers (gauche PA and water) and the complexes at M06/6-311++G (d, p) in the Ar matrix

	Computed ν	Scaled ν	Exp. ν	Scaled Shifts ($\nu_{complex}$- $\nu_{monomer}$)	Mode of Assignment
Monomer	3892.77(52)	3649.47	3649.41		O-H stretch PA
	3451.24(50)	3319.75, 3316.99	3319.86, 3317.01		C-H acetylenic stretch
	1099.13(131)	1042.52	1042.54		C-O stretch
	4015.19(84)	3775.48	3775.64		O-H asym. H_2O
	3891.78(17)				O-H sym. H_2O
Complex 1	3716.27(287)	3482.48	3512.09	-167	O-H stretch PA
	3446.59(52)	3315.27, 3312.48		-4, -4	C-H acetylenic stretch
	1119.49(125)	1061.39	1055.96	+19	C-O stretch
	3972.97(157)	3735.78		-40	O-H asym. H_2O
	3809.17(143)				O-H sym. H_2O
Complex 2	3890.50(60)	3647.34		-2	O-H stretch PA
	3450.36(54)	3318.90, 3316.14		-1, -1	C-H acetylenic stretch
	1082.05(122)	1026.32		-16	C-O stretch
	3979.99(135)	3742.38		-33	O-H asym. H_2O
	3767.37(311)				O-H sym. H_2O
Complex 3	3728.16(273)	3495.15	3512.09	-154	O-H stretch PA
	3446.24(53)	3314.94, 3312.18		-5, -5	C-H acetylenic stretch
	1121.35(123)	1063.60	1055.96	+21	C-O stretch
	3973.82(154)	3736.58		-39	O-H asym. H_2O
	3810.43(147)				O-H sym. H_2O
Complex 4	3893.76(53)	3650.40		+1	O-H stretch PA
	3445.22(55)	3313.96, 3311.20		-6, -6	C-H acetylenic stretch
	1103.47(135)	1046.64		+4	C-O stretch
	3982.49(144)	3744.73		-31	O-H asym. H_2O
	3833.59(88)				O-H sym. H_2O
Complex 5	3896.01(50)	3652.51		+3	O-H stretch PA
	3355.55(301)	3227.70, 3225.02		-92, -92	C-H acetylenic stretch
	1095.41(129)	1039.00		-3	C-O stretch
	4004.21(105)	3765.16		-10	O-H asym. H_2O
	3883.15(28)				O-H sym. H_2O

Table 13 –Computed and scaled frequencies of the monomers (gauche PA and water) and the complexes at MP2/6-311++G (d, p) in the Ar matrix

	Computed ν	Scaled ν	Exp. ν	Scaled Shifts ($\nu_{complex}$ - $\nu_{monomer}$)	Mode of Assignment
Monomer	3885.13(41)	3649.30	3649.41		O-H stretch PA
	3502.06(55)	3319.95, 3317.15	3319.86, 3317.01		C-H acetylenic stretch
	1083.70(108)	1042.52	1042.54		C-O stretch
	4003.00(63)	3775.63	3775.64		O-H asym. H_2O
	3884.75(57)				O-H sym. H_2O
Complex 1	3765.13(275)	3536.59	3512.09	-113	O-H stretch PA
	3496.97(57)	3315.13, 3312.33		-5, -5	C-H acetylenic stretch
	1098.79(107)	1057.04	1055.96	+14	C-O stretch
	3974.65(117)	3748.90		-27	O-H asym. H_2O
	3848.61(44)				O-H sym. H_2O
Complex 2	3878.39(47)	3642.97		-6	O-H stretch PA
	3501.12(59)	3319.06, 3316.26		-1, -1	C-H acetylenic stretch
	1067.43(113)	1026.87		-16	C-O stretch
	3968.00(118)	3742.62		-33	O-H asym. H_2O
	3779.97(297)				O-H sym. H_2O
Complex 3	3774.07(246)	3544.98	3512.09	-104	O-H stretch PA
	3496.59(58)	3314.77, 3311.97		-5, -5	C-H acetylenic stretch
	1100.26(106)	1058.45	1055.96	+16	C-O stretch
	3976.20(120)	3750.35		-25	O-H asym. H_2O
	3846.40(54)				O-H sym. H_2O
Complex 4	3885.84(39)	3649.97		+1	O-H stretch PA
	3497.25(58)	3315.39, 3312.59		-5, -5	C-H acetylenic stretch
	1081.86(113)	1040.75		-2	C-O stretch
	3985.69(103)	3759.30		-16	O-H asym. H_2O
	3860.54(25)				O-H sym. H_2O
Complex 5	3884.92(39)	3649.10		0	O-H stretch PA
	3436.30(231)	3257.61, 3254.86		-62, -62	C-H acetylenic stretch
	1080.62(109)	1039.56		-3	C-O stretch
	3990.71(79)	3764.04		-12	O-H asym. H_2O
	3874.40(18)				O-H sym. H_2O

Table 14 –Computed and scaled frequencies of the monomers (gauche PA and water) and the complexes at B3LYP/6-311++G (d, p) in the Ar matrix

	Computed ν	Scaled ν	Exp. ν	Scaled Shifts ($\nu_{complex}$ - $\nu_{monomer}$)	Mode of Assignment
Monomer	3829.16(35)	3649.57	3649.41		O-H stretch PA
	3474.56(62)	3319.94, 3317.16	3319.86, 3317.01		C-H acetylenic stretch
	1044.47(109)	1042.48	1042.54		C-O stretch
	3922.33(57)	3775.63	3775.64		O-H asym. H_2O
	3817.10(9)				O-H sym. H_2O
Complex 1	3666.35(306)	3494.39	3512.09	-155	O-H stretch PA
	3469.92(66)	3315.51, 3312.73		-4, -4	C-H acetylenic stretch
	1061.60(111)	1059.58	1055.96	+17	C-O stretch
	3896.81(112)	3751.07		-25	O-H asym. H_2O
	3772.91(74)				O-H sym. H_2O
Complex 2	3823.42(46)	3644.10		-5	O-H stretch PA
	3473.52(67)	3318.95, 3316.17		-1, -1	C-H acetylenic stretch
	1030.45(126)	1028.49		-14	C-O stretch
	3891.18(101)	3745.65		-30	O-H asym. H_2O
	3690.96(438)				O-H sym. H_2O
Complex 3	3678.04(286)	3505.54	3512.09	-144	O-H stretch PA
	3469.69(66)	3315.30, 3312.51		-5, -5	C-H acetylenic stretch
	1063.40(109)	1061.38	1055.96	+19	C-O stretch
	3900.92(110)	3755.02		-21	O-H asym. H_2O
	3774.46(76)				O-H sym. H_2O
Complex 5	3828.79(33)	3649.22		0	O-H stretch PA
	3393.16(270)	3242.16, 3239.45		-78, -78	C-H acetylenic stretch
	1041.31(110)	1039.33		-3	C-O stretch
	3919.55(75)	3772.96		-3	O-H asym. H_2O
	3816.72(16)				O-H sym. H_2O

Comparing with the computed frequencies at different levels of calculation, it was observed that complex 1 and complex 3 have been seen experimentally and B3LYP calculations were very good agreement to analyse the PA-water complex features in our experiments.

4.5 AIM Analysis

AIM analysis at M06 level of calculation

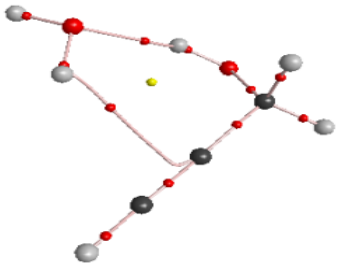

Complex 1

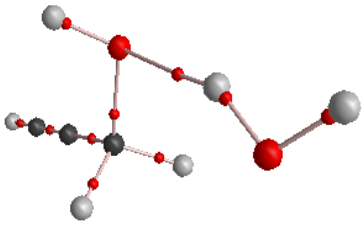

Complex 2

Complex 1	ρ (r) in a.u.	$\nabla^2\rho$ (r) in a.u.
H…π	0.0118	-0.0102
O-H…O (proton donor)	0.0248	-0.0262
Complex 2	ρ (r) in a.u.	$\nabla^2\rho$ (r) in a.u.
H-O…H (proton acceptor)	0.0240	-0.0265

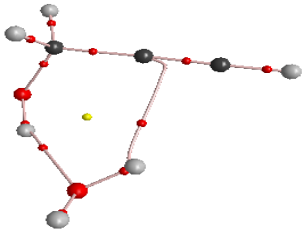

Complex 3

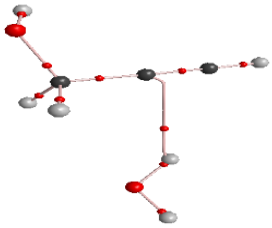

Complex 4

Complex 3	ρ (r) in a.u.	$\nabla^2\rho$(r) in a.u.
H…π	0.0121	-0.0104
O-H…O (proton donor)	0.0245	-0.0264
Complex 4	ρ (r) in a.u.	$\nabla^2\rho$(r) in a.u.
H…π	0.0124	-0.0107

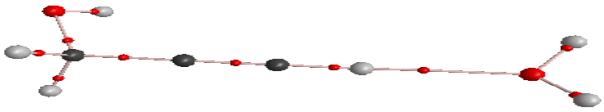

Complex 5

Complex 5	ρ (r) in a.u.	$\nabla^2\rho(r)$ in a.u.
C-H…O (proton donor)	0.0156	-0.0167

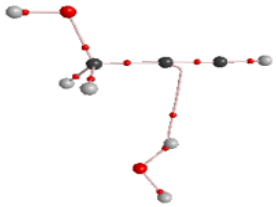

Complex 6

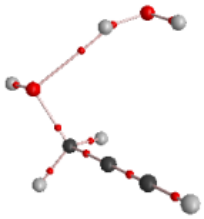

Complex 7

Complex 6	ρ (r) in a.u.	$\nabla^2\rho(r)$ in a.u.
H…π	0.0124	-0.0106
Complex 7	ρ (r) in a.u.	$\nabla^2\rho(r)$ in a.u.
H-O…H (proton acceptor)	0.0224	-0.0236

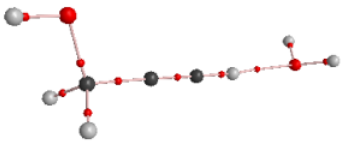

Complex 8

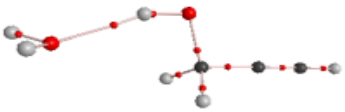

Complex 9

Complex 8	ρ (r) in a.u.	$\nabla^2\rho(r)$ in a.u.
C-H…O (proton donor)	0.0154	-0.0163
Complex 9	ρ (r) in a.u.	$\nabla^2\rho(r)$ in a.u.
O-H…O (proton donor)	0.0241	-0.0267

AIM analysis at MP2 level of calculation

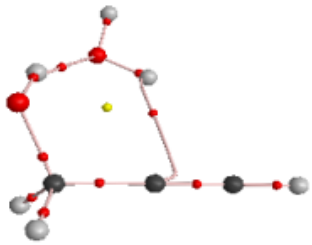

Complex 1

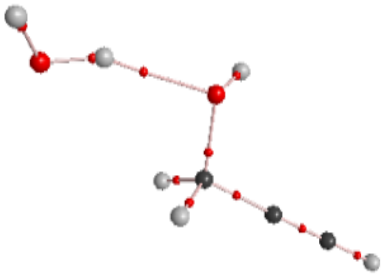

Complex 2

Complex 1	ρ (r) in a.u.	$\nabla^2\rho$ (r) in a.u.
H…π	0.0096	-0.0081
O-H…O (proton donor)	0.0233	-0.0249
Complex 2	ρ (r) in a.u.	$\nabla^2\rho$ (r) in a.u.
H-O…H (proton acceptor)	0.0236	-0.0259

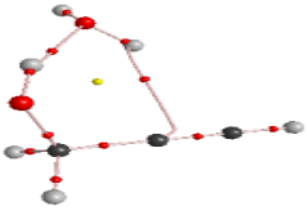

Complex 3

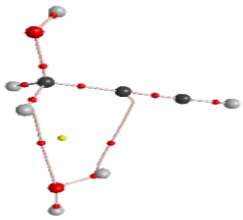

Complex 4

Complex 3	ρ (r) in a.u.	$\nabla^2\rho$(r) in a.u.
H…π	0.0104	-0.0088
O-H…O (proton donor)	0.0224	-0.0243
Complex 4	ρ (r) in a.u.	$\nabla^2\rho$(r) in a.u.
H…π	0.0100	-0.0085
H-C-H…O (proton donor)	0.0063	-0.0070

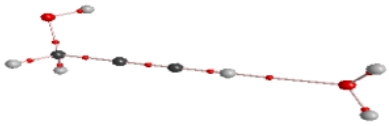

Complex 5	ρ (r) in a.u.	$\nabla^2\rho(r)$ in a.u.
C-H…O (proton donor)	0.0132	-0.0136

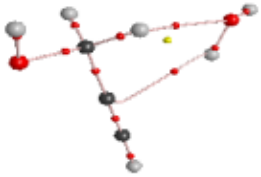

Complex6

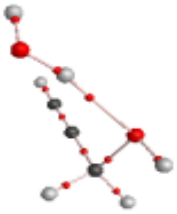

Complex 7

Complex 6	ρ (r) in a.u.	$\nabla^2\rho(r)$ in a.u.
H…π	0.0105	-0.0088
H-C-H…O (proton donor)	0.0063	-0.0068
Complex 7	ρ (r) in a.u.	$\nabla^2\rho(r)$ in a.u.
H-O…H (proton acceptor)	0.0230	-0.025

Complex 8

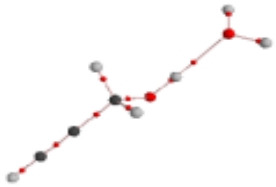

Complex 9

Complex 8	ρ (r) in a.u.	$\nabla^2\rho(r)$ in a.u.
C-H…O (proton donor)	0.0130	-0.0133
Complex 9	ρ (r) in a.u.	$\nabla^2\rho(r)$ in a.u.
O-H…O (proton donor)	0.0234	-0.0259

AIM Analysis at B3LYP level of calculation

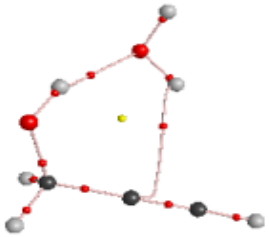

Complex 1

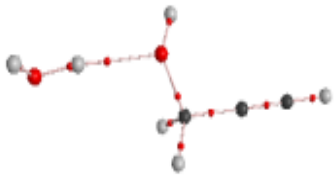

Complex 2

Complex 1	ρ (r) in a.u.	$\nabla^2\rho(r)$ in a.u.
H…π	0.0087	-0.0072
O-H…O (proton donor)	0.0235	-0.0247
Complex 2	ρ (r) in a.u.	$\nabla^2\rho(r)$ in a.u.
H-O…H (proton acceptor)	0.0236	-0.0259

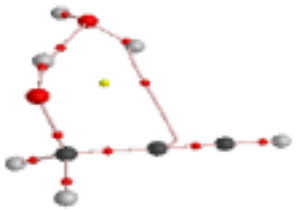

Complex 3

Complex 5

Complex 3	ρ (r) in a.u.	$\nabla^2\rho(r)$ in a.u.
H…π	0.0090	-0.0074
O-H…O (proton donor)	0.0230	-0.0247
Complex 5	ρ (r) in a.u.	$\nabla^2\rho(r)$ in a.u.
C-H…O (proton donor)	0.0136	-0.0143

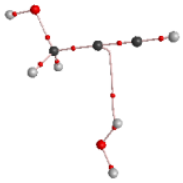

Complex 6

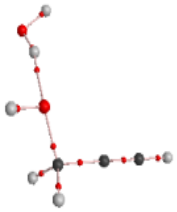

Complex 7

Complex 6	ρ (r) in a.u.	$\nabla^2\rho(r)$ in a.u.
H…π	0.0100	-0.0083
Complex 7	ρ (r) in a.u.	$\nabla^2\rho(r)$ in a.u.
H-O…H (proton acceptor)	0.0227	-0.0248

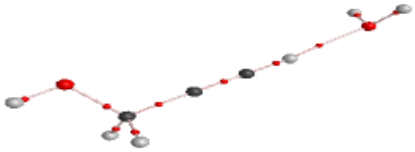

Complex 8

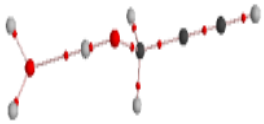

Complex 9

Complex 8	ρ (r) in a.u.	$\nabla^2\rho(r)$ in a.u.
C-H…O (proton donor)	0.0135	-0.0139
Complex 9	ρ (r) in a.u.	$\nabla^2\rho(r)$ in a.u.
O-H…O (proton donor)	0.0235	-0.0258

4.6 Vibrational assignment of trans propargyl alcohol

Table 15 - Computed frequencies of the trans propargyl alcohol at various levels of theory using 6-311++G(d,p) basis set

M06 Computed ν	MP2 Computed ν	B3LYP Computed ν	Mode of Assignment
3909.30	3883.20	3830.50	O-H stretch
3455.23	3504.37	3476.78	C-H (acetylenic) stretch
1100.98	1081.29	1044.25	C-O stretch

Table 16 - Computed frequencies of the trans propargyl alcohol-water complexes at various levels of theory using 6-311++G(d,p) basis set

M06 Computed ν	MP2 Computed ν	B3LYP Computed ν	Mode of Assignment
Complex 6			
3909.79(60)	3898.54(45)	3834.20(36)	O-H stretch PA
3444.89(54)	3499.31(57)	3473.16(65)	C-H acetylenic stretch
1104.87(143)	1080.38(122)	1045.10(127)	C-O stretch
3982.36(143)	3981.32(109)	3900.43(109)	O-H asym. H_2O
3825.94(114)	3854.88(36)	3775.01(78)	O-H sym. H_2O
Complex 7			
3898.85(73)	3875.89(53)	3823.12(48)	O-H stretch PA
3449.58(52)	3502.45(55)	3476.05(61)	C-H acetylenic stretch
1083.96(120)	1068.24(119)	1034.12(138)	C-O stretch
3962.83(80)	3967.08(92)	3892.24(84)	O-H asym. H_2O
3898.85(73)	3788.02(276)	3698.57(353)	O-H sym. H_2O
Complex 8			
3904.77(47)	3892.49(35)	3829.97(25)	O-H stretch PA
3360.34(285)	3440.89(222)	3396.65(258)	C-H acetylenic stretch
1095.65(133)	1077.55(118)	1039.76(127)	C-O stretch
4005.40(103)	3990.89(73)	3919.08(73)	O-H asym. H_2O
3883.88(28)	3874.73(18)	3816.59(16)	O-H sym. H_2O
Complex 9			
3796.36(464)	3779.45(469)	3690.46(528)	O-H stretch PA
3454.37(48)	3506.09(52)	3478.23(61)	C-H acetylenic stretch
1118.41(126)	1096.71(108)	1061.71(121)	C-O stretch
4002.00(122)	3986.93(95)	3914.07(89)	O-H asym. H_2O
3884.42(17)	3873.08(11)	3813.90(14)	O-H sym. H_2O

CHAPTER 5
SUMMARY AND CONCLUSIONS

==========

This thesis presents the study of the hydrogen bonded complexes of propargyl alcohol with water. The complexes were studied experimentally, using matrix isolation infrared spectroscopy and the experimental data were corroborated using ab initio computations. A detailed account of the spectroscopy of propargyl alcohol in Ar and N_2 matrixes has been provided. The spectral features of the dimer in both Ar and N_2 matrixes have also been assigned and discussed.

Correlation between experimental quantities such as vibrational frequencies of the various modes in the complex and computationally derived properties such as stabilization energies, charge densities at critical points on electron density topology and structural parameters have been deduced to provide a link between computational and experimental quantities.

The ground state geometry of the propargyl alcohol-water complexes is almost same on M06, MP2 and B3LYP level, which are Complex 1 and Complex 3. It has been analysed computationally that there are two interactions possible in both these minimum structure obtained at the M06, MP2 and B3LYP levels. One involves the interaction between H atom of water molecule and acetylenic π cloud of propargyl alcohol and another between O-H group of propargyl alcohol and O atom of water molecule. The cyclic geometry of the complex has been confirmed by Atoms in Molecule theory, which showed a ring critical point. At all levels, the main interaction is between O-H group of propargyl alcohol and O atom of water molecule.

5.1 Scope for future work

My work on hydrogen bonded interaction of propargyl alcohol showed that one could trap its complexes experimentally. However in this thesis, we restrict our studies to only the ground state conformer that is the gauche form. Matrix isolation infrared studies on the higher conformer (trans) would also probably show interesting results and worth studying this conformer computationally as well as experimentally. I also have performed some computational work to obtain the optimized geometries and frequencies of trans propargyl alcohol with water, which will be of great help for further studies. We can further enquire the signature of presence of trans form by complex formation.

BIBLIOGRAPHY

1 Nishio,M.; Hirota, M.; Umezawa, Y . The CH/π interaction evidence, Nature and Consequences, Wiley-VCH, New York, **1998**.

2 Whittle, E.; Dows, D.A.; Pimentel, G.C.J. Chem. Phys. **1954**,22,1943.

3 E.Hirota, J.Mol.Spectrosc. **1968**, 26 , 335-350.

4 K.Bolton, N.L. Owen, J.Sheridan, Nature **1968**, 217, 164.

5 R. A. Nyquist,Spectrochim. Acta, Part A, 1**971**, 27, 2513–2523.

6 J.C. Pearson, B.J. Drouin, J. Mol. Spectrosc. **2005**, 234, 149-156.

7 K. Bolton, J. Sheridan, Spectrochim. Acta Part A **1970**, 26, 1001 – 1006.

8 A. M. Mirri, F. Scappini, R. Cervellati, P. G. Favero, J. Mol. Spectrosc. **1976**, 63, 509 – 520.

9 A. M. Mirri, F. Scappini, H. Mader, J. Mol. Spectrosc. **1975**, 57, 264 – 270.

10 F. Scappini, P. G. Favero, R. Cervellati, Chem. Phys. Lett. **1975**, 33, 499 –501.

11 H. Møllendal, A. Konovalov, J.-C. Guillemin, J. Phys. Chem. A **2010**, 114, 5537 – 5543.

12 B. J. Miller, J. R. Lane, H. G. Kjaergaard, Phys. Chem. Chem. Phys. **2011**, 13, 14183 – 14193.

13 E. L. Stewart, U. Mazurek and J. P. Bowen,J. Phys. Org. Chem., **1996**,9, 66–78.

14 Malinovsky, A. L.; Makarov, A. A.; Ryabov, E. A. JETP **2008**, 106, 34.

15 Malinovsky, A. L.; Doljikov, Yu. S.; Makarov, A. A.; Ogurok, N. D. D.; Ryabov, E. A.Chem. Phys. Lett. **2006**, 419, 511.

16 Hudspeth, E.; McWhorter, D. A.; Pate, B. H.J. Chem. Phys.**1998**, 109, 4316.

17 Green, D.; Holmberg, R.; Lee, C. Y.; McWhorter, D. A.; Pate, B. H. J. Chem. Phys.**1998**, 109, 4407.

18 Yoo, H. S.; McWhorter, D. A.; Pate, B. H.J. Phys. Chem. A **2004**, 108, 1380.

19 Makarov, A. A.; Malinovsky, A. L.; Ryabov, E. A.J. Chem. Phys. **2008**, 129, 116102.

20 Lister, D. G.; Palmieri, P.J. Mol. Struct. **1976**, 32, 355.

21 Travert, J.; Lavalley, J. C.; Chenery, D.Spectrochim. Acta, Part A **1979**, 35, 291.

22 Marshall, K. T.; Hutchinson, J. S.J. Phys. Chem. **1987**, 91, 3219.

23 Ji Hye Lee, Hyonseok Hwang, Chan Ho Kwon, and Hong Lae Kim J. Phys. Chem. A, Vol. 114, No. 5, **2010**

24 "Microwave Spectroscopic and Atoms in Molecules Theoretical Investigations on the Ar•••Propargyl Alcohol Complex: Ar•••H-O, Ar•••π, and Ar•••C Interactions" Devendra Mani and Elangannan Arunan ChemPhysChem **2013**, 14, 754 – 763.

25 dx.doi.org/10.1021/jp306961m | J. Phys. Chem. A 2012, 116, 12014−12023.

26 Whittle, Dows, and Pimentel, J. Chern. Phys. 22, 1943 (**1954**)

27 Edwin D. Beckerand George C. Pimentel The Journal of Chemical Physics 25, 224 (**1956**)

28 *Green,D.W.;Reedy,G.T. In Fourier Transform Infrared Spectroscopy;Vol. 1, Eds. J.R.Ferraro and L.J. Basile, Chap. 1; Academic Press: New York **1978**.*

29 Gaussian 09, Revision **A.1**, Frisch, M. J.; Trucks, G. W.; Schlegel, H. B.; Scuseria, G. E.; Robb, M. A.; Cheeseman, J. R.; Scalmani, G.; Barone, V.; Mennucci, B.; Petersson, G. A.; Nakatsuji, H.; Caricato, M.; Li, X.; Hratchian, H. P.; Izmaylov, A. F.; Bloino, J.; Zheng, G.; Sonnenberg, J. L.; Hada, M.; Ehara, M.; Toyota, K.; Fukuda, R.; Hasegawa, J.; Ishida, M.; Nakajima, T.; Honda, Y.; Kitao, O.; Nakai, H.; Vreven, T.; Montgomery, Jr., J. A.; Peralta, J. E.; Ogliaro, F.; Bearpark, M.; Heyd, J. J.; Brothers, E.; Kudin, K. N.; Staroverov, V. N.; Kobayashi, R.; Normand, J.; Raghavachari, K.; Rendell, A.; Burant, J. C.; Iyengar, S. S.; Tomasi, J.; Cossi, M.; Rega, N.; Millam, J. M.; Klene, M.; Knox, J. E.; Cross, J. B.; Bakken, V.; Adamo, C.; Jaramillo, J.; Gomperts, R.; Stratmann, R. E.; Yazyev, O.; Austin, A. J.; Cammi, R.; Pomelli, C.; Ochterski, J. W.; Martin, R. L.; Morokuma, K.; Zakrzewski, V. G.; Voth, G. A.; Salvador, P.; Dannenberg, J. J.; Dapprich, S.; Daniels, A. D.; Farkas, Ö.; Foresman, J. B.; Ortiz, J. V.; Cioslowski, J.; Fox, D. J. Gaussian, Inc., Wallingford CT, **2009**.

30 F. Biegle-Koning, R. F. W. Bader, W. -H. Tang, *J. Comput. Chem*. 2000, 96, 6796, AIM **2000**.

31 *Jensen, F. Chem.Phys. Letts. **1996**,261,633.*

32 *Mayer,I; Surjan, P.R. Chem. Phys. Letts. **1992**,191,497.*

33 *Schwenke, D.W.; Truhlar, D.G. J. Chem. Phys, **1985**,82,2418.*

34 *Bader, R.F.W. Atoms in Molecules- A Quantum theory ; International Series of Monographs on Chemistry, No. 22;Oxford University Press: Cladrendon **1994***

35 *Bader, R.W.F.J.Phys. Chem. A. **1998**, 102, 7314.*

36 J. Boyd and S. L. Boyd,J. Am. Chem. Soc., **1992**,114, 1652–1655.

37 E. Arunan, G. R. Desiraju, R. A. Klein, J. Sadlej, S. Scheiner, I. Alkorta, D. C. Clary, R. H. Crabtree, J. J. Dannenburg, P. Hobza, H. G. Kjaergaard, A. C. Legon and D. J. Nesbitt,Pure Appl. Chem., **2011**, 83, 1619–1637.

38 E. R. Johnson, S. Keinan, P. Mori-Sanchez, J. Contreras-Garcia, A. J. Cohen and W. Yang,J. Am. Chem. Soc., **2010**, 132, 6498–6506.

39 http://science.gsfc.nasa.gov/691/cosmicice/interstellar.html.

40 *J. A. Miller, C. F. Melius, Combust. Flame **1992**, 91, 21 – 39.*

41 *M. Frenklach, Phys. Chem. Chem. Phys.**2002**, 4, 2028 – 2037.*

42 *R. S. Tranter, X. Yang, J. H. Kiefer, Proc. Combust. Inst.**2011**, 33, 259 – 265.*

43 *http://adsabs.harvard.edu/abs/2013mss..confEFC09M*

44 S. F. Boys and F. Bernardi*, Mol. Phys. 19, 553 (**1970**).*